

Proton Diffusion Weighted and Sodium MRI of Growing Intrahepatic and Subcutaneous Hepatocellular Carcinoma

A. Babsky¹, S. Ju¹, S. Bennett¹, B. Atthe¹, B. George¹, G. McLennan¹, and N. Bansal¹

¹Radiology, Indiana University, Indianapolis, Indiana, United States

Introduction

Hepatocellular carcinoma (HCC) growth is associated with structural and metabolic transformations that can be monitored by non-invasive ²³Na and ¹H MRI. Changes in water apparent diffusion coefficient (ADC) and total tissue Na⁺ reflect mostly alterations in relative extracellular space (ECS) in tumor tissue, while changes in intracellular Na⁺ reflect physiologic and metabolic transformation in HCC cells. Water ADC measurement in the rat intrahepatic (IH) HCC model is challenging due to the effects of respiratory, cardiac, and other physiologic motion. To reduce motion artifact, the water ADC in rodent models has been usually studied using subcutaneous (SC) tumor models, and thus the absolute ADC values of IH HCC and their post-treatment changes remain unclear. In this study, in growing IH and SC HCC rat tumors and surrounding normal tissues, we examined the relationship between 1) water ADC measured by diffusion-weighted (DW) ¹H MRI, 2) total tissue Na⁺ measured by single-quantum (SQ) ²³Na MRI, and 3) intracellular Na⁺ measured by triple-quantum-filtered (TQF) ²³Na MRI.

Methods

For the IH HCC model, one million N1S1 cells were inoculated in the left lateral lobe of the liver; for the SC HCC model, ten million cells were inoculated under the skin on the thigh. MR images were acquired with a Varian 9.4-T, 31-cm horizontal bore system. Each animal was examined weekly for 4 weeks after tumor cell inoculation. Water ADC of the IH tumors and nearby liver tissue was measured with a 63-mm birdcage coil. A multi-slice DW ¹H imaging sequence with the following imaging parameters was used: 1,100 ms repetition time (TR), 21 ms echo time (TE), 256 x 128 data points over a 80 x 80 field of view (FOV), 0.5 mm slice thickness, 1.5 mm slice gap, and $b = 0, 256, 945, \text{ and } 1,679 \text{ s/mm}^2$. Respiratory gating was used to minimize the motion effect on water ADC in IH HCC. ²³Na images of IH HCC were obtained with a loop-gap volume resonator (inner diameter = 60 mm, depth = 25 mm) tuned to 105 MHz. A 3D gradient-echo ²³Na imaging sequence with the following parameter was used: ~ 240 μs non-selective excitation RF pulse, 50 ms TR, 4.6 ms TE, 64 x 64 x 16 data points over a 60 x 60 x 36 mm FOV, and 10 min total data collection time. TQF ²³Na MRI was performed using the same parameters as for SQ ²³Na MRI, except a TR of 100 ms and a data size of 64 x 32 x 8 was used. ¹H and ²³Na MRI of SC tumors and nearby tissue were obtained with a 30 mm diameter dual-tuned loop-gap volume coil. DW ¹H, and SQ and TQF ²³Na images of SC tumor were acquired employing the same parameters as for IH tumors, except a 60 x 60 mm FOV was used. Total data collection time for a set of DW ¹H MRI, SQ ²³Na MRI, and TQF ²³Na MRI was 15, 7, and 45 min, respectively.

Results

The tumor doubling time was 3.9 days for IH HCC and 11.2 days for SC HCC (Fig. 1). Seven days after cell inoculation, the water ADC in IH HCC ($1.4 \pm 0.1 \times 10^{-3} \text{ mm}^2/\text{s}$) was significantly higher compared to the adjacent normal liver ($1.0 \pm 0.1 \times 10^{-3} \text{ mm}^2/\text{s}$, $p \leq 0.05$). This difference was consistent despite a small decrease in the ADC of IH HCC from day 7 through day 28. The motion artifacts in DW MRI were only partially avoided by respiratory gating. Fig. 2 shows that ¹H images of IH tumor can be moderately (A) or intensively (B) blurred by motion at non-zero b -values, in contrast to SC tumors (C). The water ADC of SC HCC increased from $0.63 \pm 0.01 \times 10^{-3} \text{ mm}^2/\text{s}$ at day 14 to $0.72 \pm 0.04 \times 10^{-3} \text{ mm}^2/\text{s}$ at day 21, and $0.79 \pm 0.06 \times 10^{-3} \text{ mm}^2/\text{s}$ at day 28 ($p < 0.05$ vs. 14 day value). The water ADC of SC HCC was lower ($p < 0.01$) compared to the IH HCC by 53%, 37%, and 24% on days 14, 21, and 28, respectively. Growth of IH HCC was associated with increases in both SQ and TQF ²³Na signal intensity (SI). At day 28, mean SQ ²³Na SI from the IH HCC increased to 2.5 ± 0.6 times the day 7 value ($p < 0.05$), while the SI from the surrounding liver tissue remained unchanged. The changes in TQF ²³Na were similar to SQ ²³Na but more profound. On day 21, the mean TQF ²³Na SI increased to 2.1 ± 0.5 times the day 7 value ($p < 0.05$), and on day 28 to 2.7 ± 0.5 times the day 7 value ($p < 0.05$). SC HCC tumors also showed similar changes in SQ and TQF ²³Na MRI SI. On day 28, the mean SQ ²³Na SI increased to 1.5 ± 0.1 times the day 14 value (Fig. 3). On day 21, the mean TQF ²³Na SI increased to 1.7 ± 0.4 times the day 14 value ($p < 0.05$) and on day 28 to 1.8 ± 0.4 times the day 14 value ($p < 0.05$).

Discussion

Our previous data show that the increase in SQ and TQF ²³Na MR SI of SC-implanted RIF-1 and 9L tumors are caused by increases in ECS and intracellular Na⁺ concentration, and not by changes in ²³Na relaxation times [1, 2]. Histological analysis of IH HCC showed that its growth is associated with increased inflammation and necrosis, which leads to increases in ECS and SQ ²³Na SI. The observed increase in TQF ²³Na SI may result from progressive hypoxia with tumor growth. Hypoxia shifts the tumor metabolism from oxidative phosphorylation to glycolysis, which may reduce ATP production. The decrease in energy status may decrease the activity of Na⁺/K⁺-ATPase and increase intracellular Na⁺ concentration. Thus, the observed increase in SQ ²³Na in growing HCC reflects an increase in ECS, and the increase in TQF ²³Na represents an increase in intracellular Na⁺ concentration.

Conclusion

Water ADC of HCC depends on tumor location and is greatly affected by physiological motion. SQ and TQF ²³Na MRI are not affected by motion, and show increases in total and intracellular Na⁺ with untreated tumor growth in both IH and SC tumors. SQ and TQF ²³Na MRI techniques are more reliable compared to water ADC measurements for hepatic tumor studies because of their insensitivity to motion.

References

- 1) Winter et al. *Cancer Res* 2001; 61: 2002-2007.
- 2) Babsky et al. *Neoplasia* 2005; 7: 7658-7666.

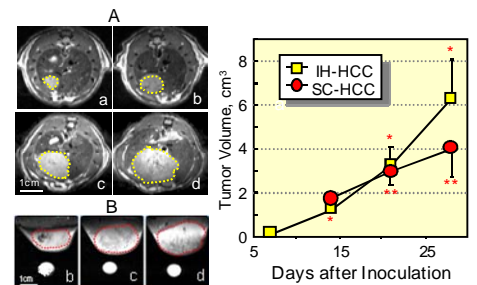


Fig. 1. The HCC volumes on 7 (a), 14 (b), 21 (c) and 28 (d) days after N1S1 cell inoculation. On the left side DWI of IH (A) and SC (B) tumors are marked by dotted lines; on the right side the means of tumor volume are presented: * $p < 0.05$ (vs. Day 7), ** $p < 0.05$ (vs. Day 14), N=5.

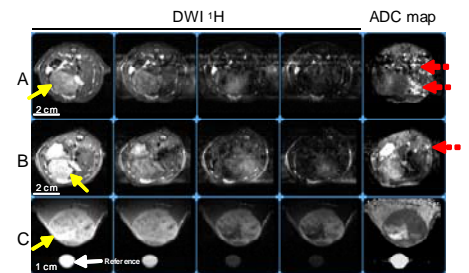


Fig. 2. DWI and ADC maps of IH (A, B) and SC (C) HCCs at different b -factors (in s/mm^2): a – 0, b – 256, c – 945, d – 1679. HCC is marked by yellow arrows and the motion artifact is marked by the dotted red arrows on the ADC maps.

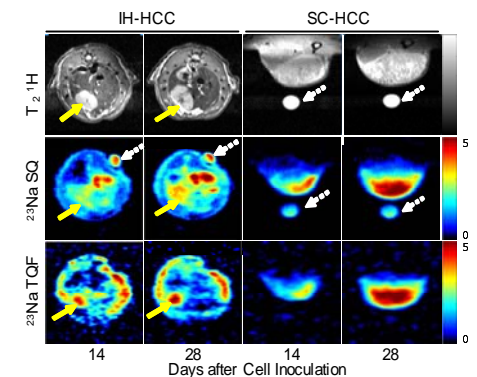


Fig. 3. DWI ¹H, SQ and TQF ²³Na MRIs of IH and SC HCCs 14 and 28 days after N1S1 cell inoculation. IH-HCCs are marked by yellow arrows and the references are marked by the dotted white arrows.